This is a repository copy of *Immunomodulatory activity of electrospun polyhydroxyalkanoate fiber scaffolds incorporating olive leaf extract*.

White Rose Research Online URL for this paper:
https://eprints.whiterose.ac.uk/174588/

Version: Published Version

Article:

De la Ossa, J.G., Fusco, A., Azimi, B. et al. (10 more authors) (2021) Immunomodulatory activity of electrospun polyhydroxyalkanoate fiber scaffolds incorporating olive leaf extract. Applied Sciences, 11 (9). 4006. ISSN 2076-3417

https://doi.org/10.3390/app11094006

Immunomodulatory Activity of Electrospun Polyhydroxyalkanoate Fiber Scaffolds Incorporating Olive Leaf Extract

Jose Gustavo De la Ossa [1,2], Alessandra Fusco [3,4], Bahareh Azimi [3,5], Jasmine Esposito Salsano [1,6], Maria Digiacomo [6,7], Maria-Beatrice Coltelli [3,5], Karen De Clerck [8], Ipsita Roy [9], Marco Macchia [6,7], Andrea Lazzeri [5], Giovanna Donnarumma [3,4], Serena Danti [5,*] and Rossella Di Stefano [2,7]

[1] Doctoral School in Life Sciences, University of Siena, 53100 Siena, Italy; josegustavo.delao@student.unisi.it (J.G.D.l.O.); ja.espositosalsano@student.unisi.it (J.E.S.)
[2] Cardiovascular Research Laboratory, Department of Surgical, Medical and Molecular Pathology and Critical Care Medicine, University of Pisa, 56126 Pisa, Italy; rossella.distefano@unipi.it
[3] Consorzio Interuniversitario Nazionale per la Scienza e Tecnologia dei Materiali (INSTM), 50121 Florence, Italy; alessandra.fusco@unicampania.it (A.F.); b.azimi@ing.unipi.it (B.A.); maria.beatrice.coltelli@unipi.it (M.-B.C.); giovanna.donnarumma@unicampania.it (G.D.)
[4] Department of Experimental Medicine, University of Campania "Luigi Vanvitelli", 80138 Naples, Italy
[5] Department of Civil and Industrial Engineering, University of Pisa, 56122 Pisa, Italy; andrea.lazzeri@unipi.it
[6] Department of Pharmacy, University of Pisa, 56126 Pisa, Italy; maria.digiacomo@unipi.it (M.D.); marco.macchia@unipi.it (M.M.)
[7] Interdepartmental Research Center "Nutraceuticals and Food for Health", University of Pisa, 56100 Pisa, Italy
[8] Centre for Textile Science and Engineering, Department of Materials, Textiles and Chemical Engineering, University of Gent, 9000 Gent, Belgium; Karen.DeClerck@UGent.be
[9] Department of Materials Science & Engineering, Kroto Research Institute, University of Sheffield, Sheffield S10 2 TG, UK; i.roy@sheffield.ac.uk
[*] Correspondence: serena.danti@unipi.it

Featured Application: We produced polyhydroxyalkanoate (PHA) ultrafine fiber meshes incorporating olive leaf extract (OLE), which is rich in polyphenols entitled with antioxidant activity. The unique PHA chemistry, small size and surface topography of electrospun fibers, together with OLE, showed immunomodulatory properties towards skin keratinocytes in vitro. OLE/PHA fiber meshes showed promise for application as tissue engineering dressings in chronic wound repair.

Abstract: Olive tree is a well-known source of polyphenols. We prepared an olive leaf extract (OLE) and characterized it via high performance liquid chromatography (HPLC) analysis. OLE was blended with different polyhydroxyalkanoates (PHAs), namely, poly(hydroxybutyrate-co-hydroxyvalerate) (PHBHV) and polyhydroxybutyrate/poly(hydroxyoctanoate-co-hydroxydecanoate) (PHB/PHOHD), to produce fiber meshes via electrospinning: OLE/PHBV and OLE/ (PHB/PHOHD), respectively. An 80–90% ($w/w\%$) release of the main polyphenols from the OLE/PHA fibers occurred in 24 h, with a burst release in the first 30 min. OLE and the produced fiber meshes were assayed using human dermal keratinocytes (HaCaT cells) to evaluate the expression of a panel of cytokines involved in the inflammatory process and innate immune response, such as the antimicrobial peptide human beta defensin 2 (HBD-2). Fibers containing OLE were able to decrease the expression of the pro-inflammatory cytokines at 6 h up to 24 h. All the PHA fibers allowed an early downregulation of the pro-inflammatory cytokines in 6 h, which is suggestive of a strong anti-inflammatory activity exerted by PHA fibers. Differently from pure OLE, PHB/PHOHD fibers (both with and without OLE) upregulated the expression of HBD-2. Our results showed that PHA fiber meshes are suitable in decreasing pro-inflammatory cytokines and the incorporation of OLE may enable indirect antibacterial properties, which is essential in wound healing and tissue regeneration.

---

1. Introduction

Olive tree (i.e., *Olea europaea*) is one of the most ancient trees of the Mediterranean area. By virtue of its properties, olive tree derivatives have been employed in traditional medicine as botanical drugs and food supplements. In particular, olive leaf extract (OLE) has been considered for different purposes [1], for example, as an antihypertensive, antiatherogenic, anti-inflammatory, hypoglycemic or hypocholesterolemic agent [2–4]. In fact, OLE is known to be a good source of antioxidants, bioactive compounds, even including polyphenols [5,6]. Among them, the secoiridoid oleuropein is the main component of OLE, in addition to other secoiridoids derived from tyrosol structures and flavonoids. The nutraceutical properties of OLE have been attributed to secoiridoid oleuropein and its derivatives, such as hydroxytyrosol [7]. Polyphenol concentration in OLE may depend on the geographical position, type of cultivar, age of the olive tree and collection season [8,9].

In recent years, polyphenols have shown a broad range of biological activities, including anti-inflammatory and immunomodulatory actions, demonstrated both in vitro and in vivo, along with a beneficial role in many acute and chronic disorders [10–13]. Inflammation is generally defined as a response of vascularized living tissue to local injury, often induced by exogenous factors, such as pathogen aggression. The inflammatory process indeed serves to neutralize, dilute or wall off the injurious agent and promotes immune cell recruitment. In addition, endogenous factors, e.g., cancer, diabetes, arthritis, neurodegenerative diseases and cardiovascular issues, among others, concur to establish and sustain the inflammatory processes. According to many epidemiological and experimental research activities of dietary polyphenols, OLE displays the ability, proper of these natural compounds, to act on pro-inflammatory genes that encode several cytokines, in addition to their antioxidant characteristics, such as reactive oxygen species (ROS) scavenging, which overall contribute to the regulation of inflammatory pathway [9,14]. Chronic inflammation occurs when an inflammatory event is not resolved and is characterized by the presence of several immune cell types, such as macrophages, monocytes and lymphocytes. It is important to mention that a type of immune cells, the macrophages, have been demonstrated to be affected by polyphenols [15]. Upon skin damage, epidermis response leads the immune reaction by the production of pro-inflammatory, anti-inflammatory and antimicrobial (i.e., defensin) molecules by keratinocytes, which do play a role in skin immunomodulation. To repair a chronically inflamed wound, dressings are usually applied to protect and enable the healing of the wound [16]. Considering the prominent role of OLE in modulating the inflammation, it is proposed the use of new biomaterials incorporating OLE in wound healing. In this process, injured epithelial cells can trigger the inflammatory response and ultimately modulate it [17].

Among the variety of biocompatible and biodegradable polymers, polyhydroxyalkanoates (PHAs), are an emerging class of biopolyesters synthesized by various microorganisms as lipid inclusions stored within cells [18]. PHAs are a wide family of polymers and copolymers; as such, they possess diverse chemical structure, which results in a diversified range of material properties, thus showing a tunable drug delivery behavior [19]. Among PHAs, poly(hydroxybutyrate-co-hydroxyvalerate) (PHBHV) copolymer has largely been investigated in the biomedical field as it shows great potential for fabricating biomedical micro- and nano- drug carriers [20]. Electrospinning is simple method to obtain meshes of ultrafine fibers, whose size falls in the order of 1–2 microns down to 10 nanometers. Such tiny fibers mimic the fibrous arrangement of the extracellular matrix (ECM). Via electrospinning, scaffolds result typically assembled into nonwoven networks, which are deposited in random or aligned fiber orientation [21]. Overall, both OLE and PHAs are bio-based materials that comply with the circular economy and green chemistry, as OLE

extraction can be water based, and the electrospinning process usually is performed at room temperature [9,16,21–23].

In this study, after characterization of polyphenol content in OLE, two types of PHA fiber meshes incorporating OLE were produced via electrospinning and proposed as wound dressings. In particular, we used commercially available PHBHV and a blend of polyhydroxybutyrate (PHB) and poly(hydroxyoctanoate-co-hydroxydecanoate) (PHOHD) produced and characterized in laboratory. The release of OLE from PHA fibers was evaluated. To assess the biological effects of the new products in vitro, we used human dermal keratinocytes (HaCaT cell line) and investigated a panel of interleukins (ILs) involved in the inflammatory and immune response.

Developing fully bio-based scaffolds provided with immunomodulatory properties would improve the management of wounds and in particular chronic wounds.

2. Materials and Methods

2.1. Materials

Acetic acid, acetonitrile (ACN), methanol (MeOH), sodium carbonate (Na_2CO_3) were purchased from Sigma-Aldrich (Milan, Italy). The following commercial compound as analytical standards are used: gallic acid, oleuropein and p-hydroxyphenylacetic acid, purchased from Sigma-Aldrich (Milan, Italy); tyrosol, hydroxytyrosol, caffeic acid, p-coumaric acid, purchased from TCI (Zwijndrecht, Belgium); luteolin-7-O-glucoside, apigenin-7-O-glucoside and rutin, purchased from Extrasynthese (Lyon, France). Folin–Ciocalteu reagent was purchased from Merk (Darmstadt, Germany). Phosphate-buffered saline (PBS) was purchased from Sigma-Aldrich (Milan, Italy) and for each analysis was diluted 10 times. Chloroform (code: 102442), 2-butanol (code: 109630), lithium bromide ($LiBr_2$), acetic acid (code: 33209), ethanol (EtOH), PHBHV (HV content 12% *w/v*) and Dulbecco's phosphate-buffered saline (DPBS) were provided by Sigma-Aldrich (Milan, Italy). Immortalized human keratinocytes, HaCaT cell line was purchased from CLS—Cell Lines Service, Eppelheim, Germany. $MgCl_2$, Dulbecco's Modified Essential Medium (DMEM), L-glutamine, penicillin, streptomycin and fetal calf serum were purchased from Invitrogen, (Carlsbad, CA, USA). AlamarBlue was bought from Thermo Fisher Scientific (Waltham, MA, USA). LC Fast Start DNA Master SYBR Green kit was obtained from Roche Applied Science (Euroclone S.p.A., Pero, Italy). P(3HB) and P(3HO-3HD) were supplied by Roylab, University of Sheffield, UK.

2.2. OLE Extraction

Olive leaves were obtained from *Olivastra seggianese* plantation located at CNR-IVALSA, Follonica (GR), Italy. Leaf collection was manually performed in May 2019. Following liquid nitrogen freezing and hand-made crushing, the leaves powder was added with water and sonicated followed by vortex mixing. After centrifugation at 4000 rpm for 5 min, at 25 °C, the water phase was filtered and freeze-dried obtaining OLE.

2.3. OLE Characterization

A high-performance liquid chromatography analysis (HPLC) was carried out to identify and quantify the major phenolic compounds of the OLE using a slightly modified method developed in a previous study [24]. The retention times and UV absorbance spectra of phenolic compounds present in OLE were compared with those of the commercial standard and quantified at 278 nm, using p-hydroxyphenyl acetic acid as the internal standard, according to the previously reported method [9]. Sample concentrations were determined by linear regression. For each calibration curve, the correlation coefficients were >0.99. HPLC analysis was performed with a HPLC instrument (Thermo Finnigan-Spectra System SCM1000) equipped with a Spectra System P2000 (Pumps), Spectra System UV2000, set to 280 nm, and using a Phenomenex Gemini reverse-phase C18 column (250 × 4.6 mm, 5 μm particle size; Phenomenex, Castel Maggiore, Italy). The mobile phase was a mixture of H_2O/acetic acid (97.5:2.5 *v/v*) (A) and ACN (B). A linear gradient was run

from 5% (B) to 25% (B) in 20 min; it changed to 50% (B) during 20 min (40 min total time); in 10 min it changed to 80% (B) (50 min total time), after re-equilibration in 5 min (55 min, total time) to initial composition. The flowrate was 1 mL/min, and the injected volume was 50 μL. Samples were injected as a mixture of methanol/PBS (1:1 *v*/*v*). To assess the phenol content, 10 mg of OLE powder was dissolved in PBS and therefore analyzed with HPLC. The amount of phenolic compounds incorporated inside the polymer fibers was investigated using 4 cm^2 square meshes dissolved in MeOH, and the resulting solution was analyzed by HPLC.

The total phenolic (TP) content was determined using the Folin–Ciocalteu method and gallic acid as the standard equivalent (ug GAE /mg), following a reported procedure [25]. About 10 mg of OLE were dissolved in 10 mL of CH_3OH-H_2O (80:20 *v*/*v*), and then, an aliquot of this solution (1 mL) was mixed with 0.25 mL of Folin–Ciocalteu reagent and 1.5 mL of Na_2CO_3 (20% *w*/*v*). After purified water was added to reach the volume of 10 mL, the resulting mixture was kept for 45 min at the controlled temperature of 25 °C. Spectrophotometric analysis was performed at λ = 725 nm.

2.4. Scaffold Fabrication

PHAs were used to prepare blends with OLE to be processed via electrospinning: (a) commercial PHBHV and (b) a blend of P(3HB)/P(3HO-3HD) (laboratory made). Different solutions were set up for optimizing PHA the electrospinning process (Linari Engineering s.r.l, Pisa, Italy): (1) PHBHV was dissolved in a dichloromethane/methanol (10:1 *w*/*w*) mixture at 15% *w*/*w*.; (2) P(3HO-3HD)/(PHB) 10:1 (*w*/*w*) was dissolved in chloroform/2-butanol (7:3 *w*/*w*) mixture and 0.002 g/mL LiBr at 11% *w*/*w*. OLE (16.8 w%) was added to both solutions. Parameters of electrospinning were 40 kV, 0.5 mL/h flow rate and a distance from needle tip (ground charge) to static aluminum collector (positive charge) of 40 cm for 1 h. Humidity was maintained at 40% and temperature 20 °C throughout.

2.5. Phenol Release

To investigate the release of phenols from the fibers, the diffusion of phenolic compounds in PBS as a release medium was determined. A 4 cm^2 square-shaped PHBHV/OLE was inserted into a 3 cm diameter well of a multi-well plate, and 2 mL of PBS was added to each well. Then, the plate containing the solutions was incubated in an oven at a controlled temperature of 37 °C. At defined time intervals (i.e., 0, 0.5, 1, 1.5, 3, 4, 6, 24 h) medium was removed, the well was washed with 1 mL of PBS, and an equal amount of the fresh medium (2 mL) was replaced each time [26,27]. The qualitative-quantitative evaluation of the phenols released from the fiber was carried out by HPLC analysis.

2.6. Epidermal Cell Culture and Metabolic Assay

Immortalized human keratinocytes (HaCaT cells) were cultured in DMEM supplemented with 1% Penstrep, 1% glutamine and 10% fetal calf serum inside a humidified incubator set at 37 °C in air and 5% CO_2. The HaCaT cells, seeded inside 12-well plates until 80% of confluence, were incubated for 24 h with the PHA fiber meshes or OLE alone and considered as samples (s). Control experiments (c) were performed by adding the dye in well plates without the cells. At the end of this time, AlamarBlue dye was added according to the manufacturer's instructions and incubated for 4 h. The monolayer cultures received the same amount of OLE present in the OLE/PHA counterparts, which was calculated by weighting the OLE/PHA samples. The absorbance (λ) of supernatants was measured with a spectrophotometer (Victor 3; PerkinElmer, Waltham, MA, USA) under a double wavelength reading (570 nm and 600 nm). Finally, the dye reduction percentage (%AB_{red}) was calculated correlating the absorbance values and the molar extinction coefficients of the dye at the selected wavelengths, following the protocol provided by the manufacturer.

The equation (Equation (1)) applied is shown below, in which: λ = absorbance, s = sample, and c = control:

$$\%AB_{red} = 100 \cdot \frac{\left(117{,}216 \cdot \lambda_{s(570\ nm)} - 80{,}586 \cdot \lambda_{s(600\ nm)}\right)}{\left(155{,}677 \cdot \lambda_{c(600\ nm)} - 14{,}652 \cdot \lambda_{c(570\ nm)}\right)} \tag{1}$$

2.7. Evaluation of Immunomodulatory Properties

The immunomodulatory properties were assayed using HaCaT cell line. The cells, cultured as described above, seeded inside 12-well plates until 80% of confluence, were incubated with the PHA fiber meshes for 6 and 24 h (n = 3). At these endpoints, total RNA was isolated with TRizol, and 1 µm of RNA was reverse-transcribed into complementary DNA (cDNA) using random hexamer primers, at 42 °C for 45 min, according to the manufacturer's instructions. Real time polymer chain reaction (PCR) was carried out with the LC Fast Start DNA Master SYBR Green kit using 2 µL of cDNA, corresponding to 10 ng of total RNA in a 20 µL final volume, 3 mM MgCl$_2$ and 0.5 µM sense and antisense primers (Table 1). Real-Time PCR was used to evaluate the expression of IL-1α, IL 1β, IL-6, IL-8, tumor necrosis factor alfa (TNF-α) and transforming growth factor beta (TGF-β).

Table 1. Real-time PCR primer sequence and operating conditions for HaCaT cells.

Gene	Primer Sequence	Conditions	Base Pairs
IL-1α	5′-CATGTCAAATTTCACTGCTTCATCC-3′ 5′-GTCTCTGAATCAGAAATCCTTCTATC-3′	5 s at 95 °C, 8 s at 55 °C, 1 s at 72 °C for 45 cycles	421
IL-1β	5′-GCATCCAGCTACGAATCTCC-3′ 5′-CCACATTCAGCACAGGACTC-3′	5 s at 95 °C, 14 s at 58 °C, 28 s at 72 °C for 40 cycles	708
TNF-α	5′-CAGAGGGAAGAGTTCCCCAG-3′ 5′-CCTTGGTCTGGTAGGAGACG-3′	5 s at 95 °C, 6 s at 57 °C, 13 s at 72 °C for 40 cycles	324
IL-6	5′-ATGAACTCCTTCTCCACAAGCGC-3′ 5′-GAAGAGCCCTCAGGCTGGACTG-3′	5 s at 95 °C, 13 s at 56 °C, 25 s at 72 °C for 40 cycles	628
IL-8	5′-ATGACTTCCAAGCTGGCCGTG-3′ 5′-TGAATTCTCAGCCCTCTTCAAAAACTTCTC-3′	5 s at 94 °C, 6 s at 55 °C, 12 s at 72 °C for 40 cycle	297
TGF-β	5′-CCGACTACTACGCCAAGGAGGTCAC-3′ 5′-AGGCCGGTTCATGCCATGAATGGTG-3′	5 s at 94 °C, 9 s at 60 °C, 18 s at 72 °C for 40 cycles	439
hBD-2	5′-GGATCCATGGGTATAGGCGATCCTGTTA-3′ 5′-AAGCTTCTCTGATGAGGGAGCCCTTTCT-3′	5 s at 94 °C, 6 s at 63 °C, 10 s at 72 °C for 50 cycles	198

2.8. Statistical Analysis

Statistical analysis was carried out by SPSS (SPSS v.21.0; IBM) and shown as mean ± standard deviation (SD). For PCR analysis, each marker expression level was compared against its untreated control using Student's t-test. Probability (p) values < 0.05 were considered as statistically significant differences.

3. Results

3.1. OLE Characterization

The TP content of OLE was estimated via the Folin–Ciocalteu method, resulting in 58.47 µg GAE/mg. Furthermore, HPLC analysis allowed to determine the main phenolic compounds present in OLE, which were oleuropein and luteolin-7-O-glucoside, with a concentration of 32.64 ± 3.06 mg/g of OLE and 6.97 ± 0.24 mg/g of OLE, respectively. In addition, we detected apigenin-7-O-glucoside with a concentration of 1.97 ± 0.17 mg/g of OLE, rutin with a concentration of 3.37 ± 0.33 mg/g of OLE and other compounds, such as hydroxytyrosol, caffeic acid and p-coumaric acid, with concentrations lower than 1 mg/g of OLE (Figure 1).
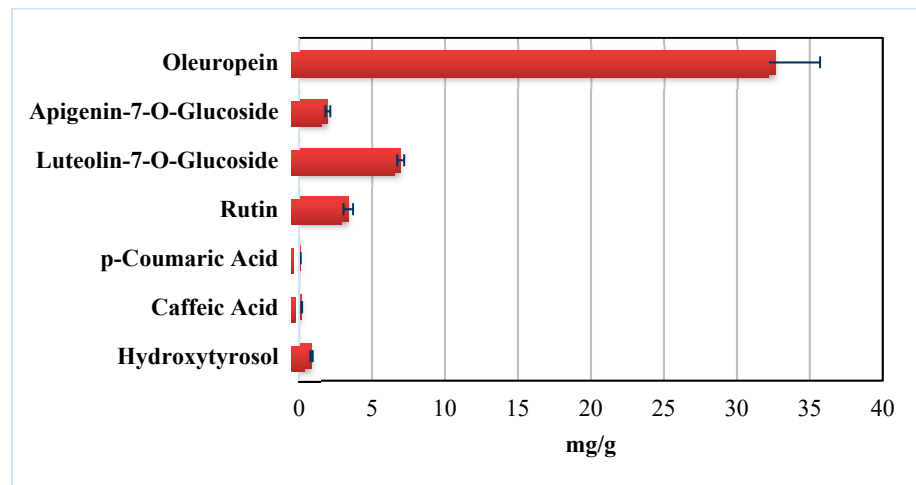
Figure 1. Bar graph showing the content (mg/g) of different phenolic compounds detected in OLE.

3.2. Morphological Characterization of PHA Fiber Meshes

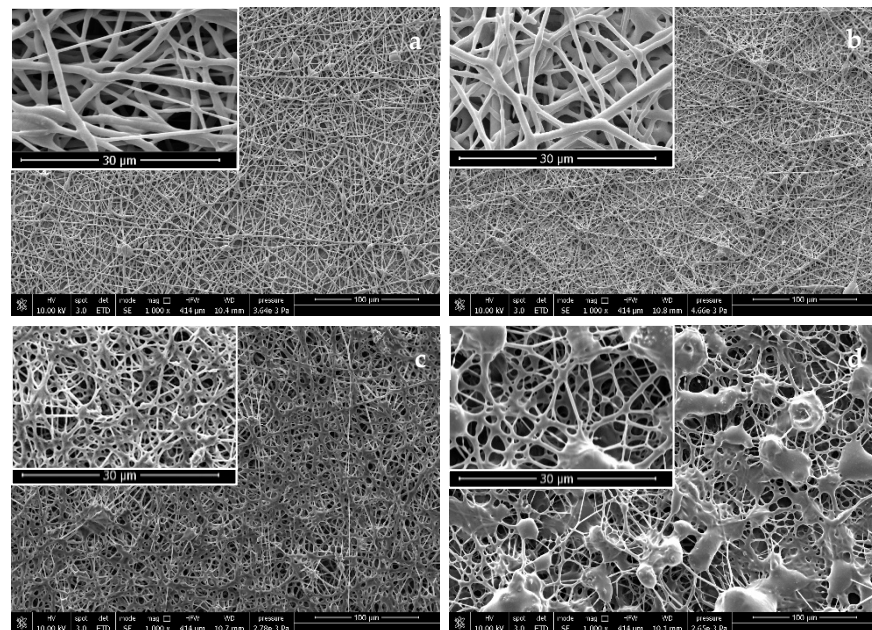Morphological features of the PHA fiber formulations were investigated via SEM (Figure 2).

Figure 2. SEM micrographs of electrospun PHA fibers: (**a**,**b**) PHBHV (commercial), and (**c**,**d**) PHB/PHOHD (from Roy's laboratory); (**a**,**c**) plain PHAs, and (**b**,**d**) PHAs incorporating OLE. Original magnification 1000× (scale bar 100 μm). Lens show details of the fibers (scale bar 30 μm).

3.3. Polyphenol Release from PHA Fibers

The phenolic content of PHBHV/OLE was analyzed. The results of HPLC analysis indicated that the amount of main phenols present was 21.84 ± 0.14 μg for oleuropein, 7.22 ± 0.78 μg for luteolin-7-O-glucoside and 3.54 ± 0.13 μg for apigenin-7-O-glucoside. Subsequently, we have evaluated the release profile of these polyphenols (oleuropein, luteolin-7-O-glucoside and apigenin-7-O-glucoside) from fiber. The quantity of these released phenolic compounds during the submersion time (24 h), as shown in Figure 3, was expressed as percentage of initial amount.
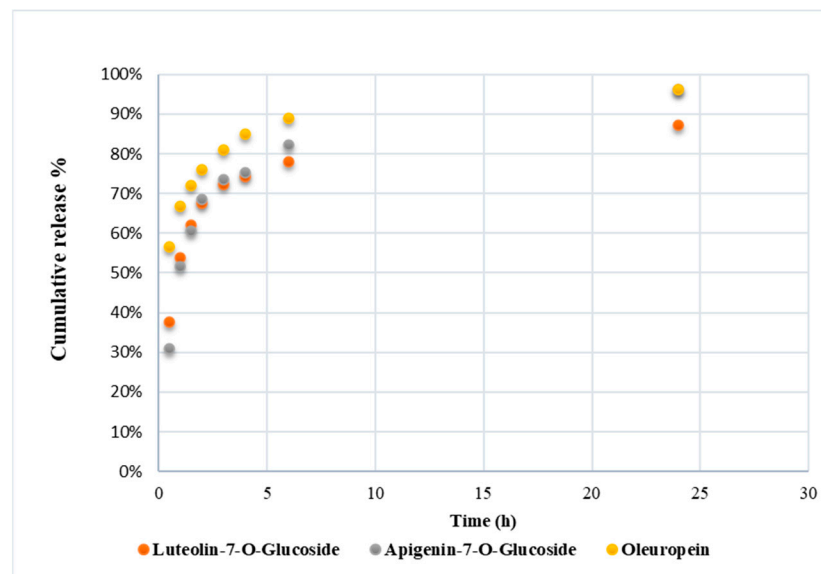
Figure 3. Graph showing the cumulative release ($w/w\%$) of the three main OLE polyphenols from PHBHV/OLE fiber meshes during 24 h. The released quantities after 6 h reached 90% ($w/w\%$) for oleuropein, and 80% ($w/w\%$) for luteolin-7-O-glucoside and apigenin-7-O-glucoside. The highest release is observed for all polyphenols during the first 30 min.

At the first 30 min, the amount of oleuropein released was about 60% of the total oleuropein content in the fiber. Then the release became more gradual, reaching about 90% after 6 h. Luteolin-7-O-glucoside and apigenin-7-O-glucoside after the first 30 min were released about 40% and 30%, respectively, with respect to the initially loaded quantity in the fibers, reaching about 80% after 6 h in both cases. Chromatograms are reported in Supplementary Materials (Figures S1–S3).

3.4. Cell Metabolic Activity

Results of metabolic activity (AlamarBlue test) performed using human dermal keratinocytes (HaCaT cells) after 24 h showed that all the samples had dye reduction percentage (%AB$_{red}$) above 70%, and remarkable differences among the fiber samples were not revealed (Table 2). Pure OLE, tested in monolayer (i.e., without the fibers) cultures showed increased metabolic activity in these cells if compared to the fiber samples. Overall, these results confirmed the good cytocompatibility of the PHAs and OLE.

Table 2. Results of metabolic activity (AlamarBlue test). Data are given as average ($n = 2$).

Sample	PHBHV Fibers	OLE/PHBHV Fibers	PHB/PHOHD Fibers	OLE/(PHB/PHOHD) Fibers	Plain OLE
%AB$_{red}$	74%	77%	76%	75%	94%

3.5. Cytokine Expression

The results for the different pro-inflammatory ILs, expressed at mRNA level from HaCaT cells in contact with the scaffolds as well as pure OLE after 6 and 24 h, are reported in Figures 4–7. OLE alone was administrated to the cells in standard culture (namely, without fibers) using the same dose loaded in 1 cm^2 of fibers. Figure 4 shows the expression of IL-1 (α and β isoforms) by HaCaT cells in contact with the different PHA fibers and with OLE up to 24 h. Comparing to the basal expression conditions of HaCaT cells, both IL-1α and IL-1β expressions were significantly downregulated by all the fibers in 6 h, independently of OLE incorporation. OLE alone was able to modulate IL-1α and IL-1β expression in 24 h, showing statistical significance in IL-1β ($p < 0.05$). The specific action of OLE in long term (24 h) downregulation of IL-1β was observed in OLE/P(PHB/PHOHD) fibers ($p < 0.05$).

Differently, plain PHBHV fibers maintained a significantly reduced expression over time ($p < 0.01$).
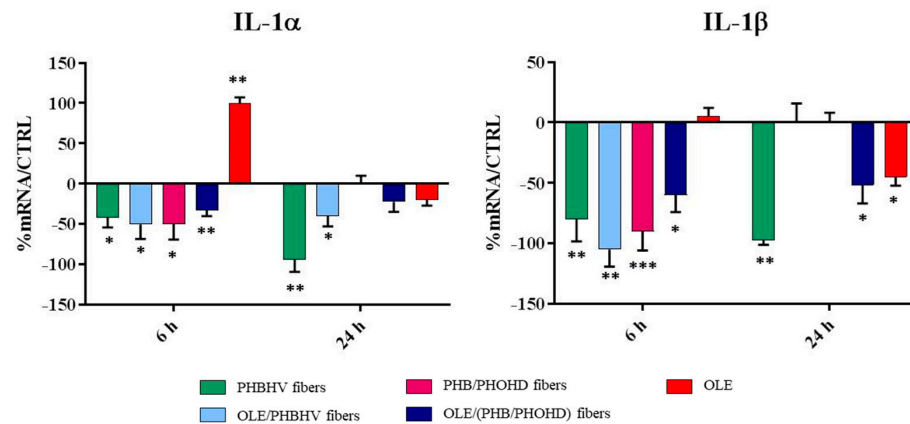

Figure 4. Bar graphs showing IL-1 expression by HaCaT cells at 6 and 24 h: IL-1α, and IL-1β. Comparisons between samples were analyzed by Student's *t*-test. Data are mean ± SD and are expressed as percentage of increment relative to untreated cells (used as controls). Significant

Figure 5. Bar graph showing IL-6 expression by HaCaT cells at 6 and 24 h. Comparisons between samples were analyzed by Student's *t*-test. Data are mean ± SD and are expressed as percentage of increment relative to untreated cells (used as controls). Significant differences are indicated by * ($p < 0.05$), ** ($p < 0.01$) and *** ($p < 0.001$) for comparison between each sample and its respective control.
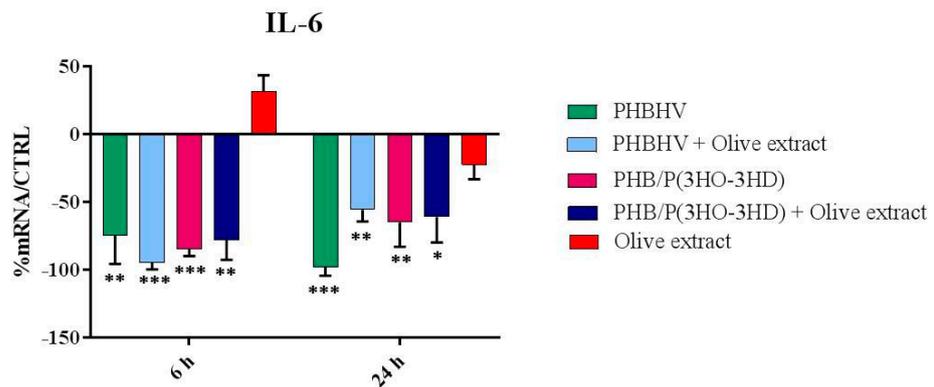

Figure 6. Bar graph showing IL-8 expression by HaCaT cells at 6 and 24 h. Comparisons between samples were analyzed by Student's *t*-test. Data are mean ± SD and are expressed as percentage of increment relative to untreated cells (used as controls). Significant differences are indicated by * ($p < 0.05$), ** ($p < 0.01$) and *** ($p < 0.001$) for comparison between each sample and its respective control.
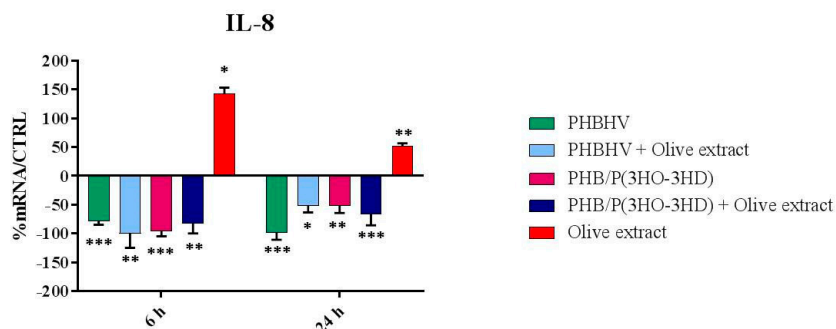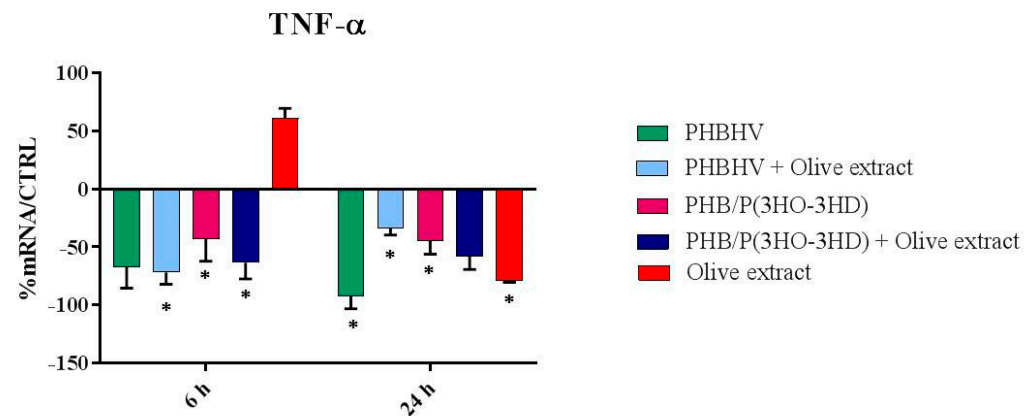
Figure 7. Bar graph showing TNF-α expression by HaCaT cells at 6 and 24 h. Comparisons between samples were analyzed by Student's *t*-test. Data are mean ± SD and are expressed as percentage of increment relative to untreated cells (used as controls). Significant differences are indicated by * (*p* < 0.05) for comparison between each sample and its respective control.

The expression of IL-6 is displayed in Figure 5. IL-6 resulted to be strongly downregulated by all the PHA fiber formulations with statistical significance (all *p* < 0.05). OLE alone did not significantly changed the IL-6 expression level at 6 and 24 h with respect to the basal expression level of HaCaT cells (*p* = n.s.). A specific effect of OLE incorporation in the fibers could not be revealed for IL-6 expression.

The outcomes of IL-8 expression are reported in Figure 6. Moreover, in this case, a strong downregulation of this cytokine was exerted by all the fibers independently of OLE incorporation (all *p* < 0.05). Differently, OLE alone caused a marked upregulation after 6 h (*p* < 0.05), which was still significant after 24 h (*p* < 0.01).

The results of TNF-α expression are shown in Figure 7. In a similar fashion to the findings reported for the other cytokines, all the PHA fibers downregulated the expression of TNF-α independently of OLE incorporation. Plain OLE was also able to downregulate the expression of this pro-inflammatory cytokine at 24 h (*p* < 0.05).

Finally, TGF-β was not modulated by any PHA and/or OLE formulation tested in this study (data not shown).

3.6. Indirect Antimicrobial Activity

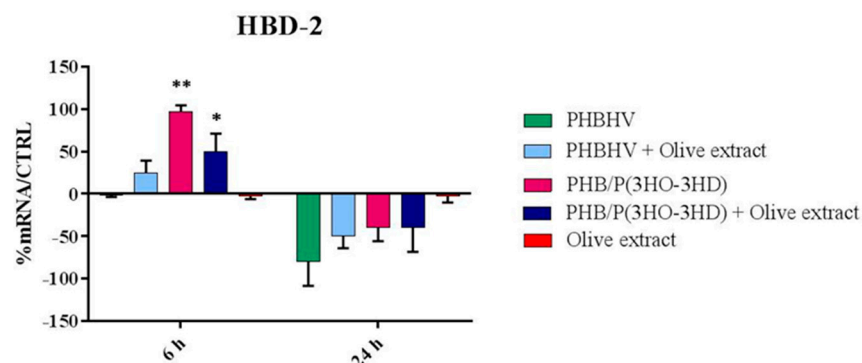The expression of the antimicrobial peptide HBD-2 is reported in Figure 8.

Figure 8. Bar graph showing HBD-2 expression by HaCaT cells at 6 and 24 h. Comparisons between samples were analyzed Student's *t*-test. Data are mean ± SD and are expressed as percentage of increment relative to untreated cells (used as controls). Significant differences are indicated by * (*p* < 0.05) and ** (*p* < 0.01) for comparison between each sample and its respective control.

In this case, it was observed that only two PHB/PHOHD fiber formulations were able to promote the upregulation of HBD-2 with statistical significance, after 6 h, specifically PHB/PHOHD containing OLE ($p < 0.05$) and plain PHB/PHOHD ($p < 0.01$). OLE/PHBHV was able to increase the expression of this peptide without statistical significance after 6 h. OLE alone, at the same concentrations, did not show any effect on HaCaT cells.

4. Discussion

Chronic wounds result from a widespread group of pathologies, including, among others, ulcers from diabetic, vascular and pressure diseases [28]. Such wounds still represent a healthcare challenge around the globe by affecting several millions of people, as they remain unhealed for months or years. Even if the underlying pathologies play a key role in wound establishment and perpetuation, chronic wounds possess some common features, defined as "*prolonged or excessive inflammation, persistent infections, formation of drug-resistant microbial biofilms, and the inability of dermal and/or epidermal cells to respond to reparative stimuli*" [28]. The possibility of modulating the inflammatory processes and improving the self-defense towards microorganisms can thus facilitate a more efficient regeneration operated by skin cells. Dressings are usually applied at the wound site to enable protection, homeostasis and absorb exudate if needed [29]. The modern wound dressings also aim to facilitate the reparatory processes by releasing growth factors or providing material-intrinsic antimicrobial properties [30].

Bioresorbable natural-origin materials offer remarkable opportunities in this field; in fact, if these biomaterials are spun into micrometric or submicrometric fibers, a structure similar to the fibrous components of ECM is provided for the neighboring cells to repair a wound [16]. To this purpose, biomaterial scaffolds stimulating immunomodulatory and antimicrobial activity in the skin cells, would offer a relevant alternative to current treatments. We hypothesized that the polyphenols present in OLE could provide a beneficial role in skin immunomodulation and that their presence in a fibrous dressing could promote their function by means of a better controlled local release to the cells within/from a three-dimensional (3D) structure.

We considered a novel family of polyesters, i.e., PHAs, as a bio-based polymer source to produce ultrafine fiber nonwovens via electrospinning. Previous studies with plain PHAs confirmed the good electro-spinnability of these polymers [31–33]. In this study, by using identical solvents and solution parameters, two types of fiber mesh were obtained: one based on commercial PHBHV and one based on a blend of two laboratory-produced PHAs, i.e., PHB/PHOHD, which were previously tested under distinct electrospinning modalities and apparatus [31–33]. Both of them were loaded with the same amount of OLE and used for in vitro tests performed using human dermal keratinocytes (HaCaT cells). We observed that the presence of OLE differently affected the final architecture of two PHA formulations, by favoring the formation of beads and molten fibers in particular in the PHB/PHOHD nonwovens. In electrospun manufacts, beads are considered as morphological defects due to nonoptimal electrospinning conditions, as the fiber diameter is not consistent along fiber length [34]. Beads result to strongly depend on surface tension, and solvents or additives can help to reduce this phenomenon [35]. However, it has been reported that in case of fibrous meshes loaded with bioactive agents, beaded structures can act as mini-reservoirs of the drug, thus enabling a better tunable delivery [36]. Similar to other parts of the olive tree, OLE contains considerable amounts of polyphenols [37]; among them, oleuropein is the key phenolic compound found in unprocessed olive fruits and also in leaves, where it reaches about 60–90 mg/g (dry weight) [38].

The well-known antioxidant activity of oleuropein is manifold: it directly relies on its chemical structure owning an ortho-diphenolic group able to scavenge reactive oxygen species (ROS) via hydrogen donation and to stabilize oxygen radicals via an intramolecular hydrogen bond. In addition, oleuropein provides an indirect antioxidant activity by stimulating the expression of intracellular antioxidant enzymes and increasing the level of nonenzymatic antioxidant molecules [38]. Recently, the anti-inflammatory properties of olive

products have also been investigated in relation to dietary food [39]. Chronic inflammation is linked to ROS production causing oxidative damage and antioxidant depletion. As such, some studies have investigated the influence of oleuropein on macrophages, the key cells involved in inflammatory processes by producing ROS and other pro-inflammatory cytokines, but further able to support healing by releasing anti-inflammatory cytokines, if timely and properly differentiated [40–42]. In some studies, OLE is reported to show direct antimicrobial activity, which was primarily attributed to its main polyphenols [43]. However, the findings available on the antibacterial properties of OLE are still debated, as they may depend on extraction methods, polyphenol composition and quantity, including dose, on selected bacteria; as such, combined technologies including for example OLE and plasma can be needed [44].

In our study, we assayed the release of three main components of OLE, namely, oleuropein, luteolin-7-O-glucoside and apigenin-7-O-glucoside from PHA fiber meshes. Such polyphenols were almost totally released after 24 h, reaching oleuropein about 90% and the two glucosides about 80% in 6 h. Unlike using systemic or even local injections, the scaffold can promote a better confined delivery at the wound site by avoiding the dispersion of the active principle through the blood vessels, thus keeping the drug concentration locally higher [45]. In addition to OLE release, it is expected that the fiber meshes would provide a suitable support for tissue regeneration. Since re-epithelization is a leading phenomenon in skin repair, we investigated the viability of HaCaT cells by measuring their metabolic activity on the different meshes, with or without OLE, including using OLE alone. We observed that, when cultured on the fibrous scaffolds for 24 h, HaCaT cell metabolic activity was very similar, independently of the type of fiber or OLE loading, whereas it was higher when pristine OLE was added at the same amount. The difference of plain OLE effect on cell metabolic activity can be explained by the subitaneous availability of the bioactive ingredients with respect to a slower release operated by the fibers. However, it is frequently observed that the presence of a three-dimensional substrate affects cell response at early time-points, as adhesion phenomena and cell–cell interactions are more complex events than in bi-dimensional tissue culture plastics [46,47].

In addition to macrophages, also epithelial cells, including skin keratinocytes, play a fundamental role in innate immunity, being primarily exposed to injuries and inflammatory stimuli. As such, epithelial cells contribute to healing by secreting several cytokines and defensins [17]. As well as for metabolic activity, the administration of OLE alone or mediated by PHA fibers after 24 h gave different outcomes in terms of cytokine expression at mRNA level. Our results showed that all the PHA fiber samples were endowed with immunomodulatory properties. In fact, they were able to downregulate the pro-inflammatory cytokines at 6 and 24 h, thus showing a suppressive function towards inflammation. Many studies have reported that cell-biomaterial surface interaction is central in biocompatibility as it rules the inflammatory process, including anti-fouling and antibacterial aspects [48]. Differently from the fiber samples, pure OLE displayed a role in the wound healing process, by modulating the expression of the pro-inflammatory cytokines, which were upregulated at 6 h and downregulated at 24 h. Wound healing is a complex process occurring via a cascade of events such as inflammation, reepithelization, matrix formation, tissue repair and remodeling. Two main phases drive this process: the first phase starts with the production of pro-inflammatory cytokines. TNF-α and IL-1 represent the primary cytokines of pro-inflammatory response, which are immediately released by keratinocytes upon wound damage. TNF-α is an essential mediator of inflammation; it evokes several responses by the vascular and coagulation systems which end up in recruiting immune cells and molecules but may also cause tissue necrosis [49]. In addition, TNF-α is able to stimulate the production of fibroblast growth factor (FGF), which can support reepithelization [50]. IL-1 has two forms, namely, IL-1α and IL-1β, respectively produced by two different genes, with structural homology of 30%, but analogous biological activity. At low doses, IL-1 promotes local inflammation and coagulation. IL-1β is the best-known form; it activates an antimicrobial pattern on the neighboring epithelial cells, contributing to the upregulation of IL-6,

which recruits and induces the differentiation of immune cells, and/or to the production of IL-8, which ultimately contributes in regulating reepithelization, tissue remodeling and angiogenesis [17,51,52]. The TGF-β is a powerful anti-inflammatory cytokine entitled with different activities, both prohibitory and stimulatory. In our finding, it was not modulated after 24 h by any tested compounds and materials.

Inflammation is described as an interaction of pro- and anti-inflammatory cytokines. Usually, chronic wounds have high levels of pro-inflammatory cytokines and underlying infections, conditions that self-sustain each other over long times, thus impeding the second phase of the healing process [53,54]. We showed that all the produced PHA fibers, either incorporating or not OLE, were able to strongly and persistently downregulate of hundred-fold differences the expression of all the above cited ILs, with respect to the basal conditions of HaCaT cells in conventional culture. It is possible that this particular polymer class, i.e., PHAs, and the architecture of the ultrafine fibrous meshes both concurred to mimic the fibrous ECM of dermal tissue produced by fibroblasts. In fact, it has been demonstrated that the smaller diameter fiber (e.g., micro-nano size) scaffolds the lesser immune response by macrophages using electrospun fibers of another polyester, the polylactide acid [55]. Regarding OLE alone, Liu et al. indicated that OLE showed a remarkable inhibitory effect on the growth of several food pathogens when administrated at 62.5 mg/mL OLE or 25 mg/mL oleuropein [39]. In our findings, the direct antibacterial effect of OLE at 100 mg/mL may still be insufficient [44]. Due to the high volume-to-surface area and porosity of electrospun fiber meshes, the resulting scaffold has a very low surface density. As such, this kind of OLE encapsulation is apt for a diffused release. Using electrospun fibers is thus inherently suitable to provide a sustained low dose delivery of OLE, which is however combined with architectural cues provided by the fibers to induce tissue regeneration. We thus investigated if these scaffolds could promote indirect (i.e., cell mediated) antibacterial activity by assaying the expression of HBD-2. In response to injury and irritation, epidermal keratinocytes secrete also antimicrobial peptides, along with cytokines and chemokines [17,56].

The family of β-defensins is composed of small cationic peptides produced by several cell types, including epithelial cells, Paneth cells, neutrophils and macrophages. These peptides possess antimicrobial activity and may be secreted constitutively or in response to microorganisms or cytokines, thus contributing to innate immunity. HBD-2 is an inducible antimicrobial peptide, reported to act as an endogenous antibiotic against Gram-positive and Gram-negative bacteria, fungi and the envelope of some viruses. Being released by epithelial cells, including epidermal keratinocytes, following inflammation, injury or infections, it is involved in the innate immune response of wounds [57]. The capability of nano/micro-structured materials of inducing HBD-2 expression in HaCaT cells has been recently reported and is considered very appealing for skin contact applications, including medical, sanitary and cosmetics [58–61]. In particular, some electrospun fibrous structures have shown promise in enabling HBD-2 by remarkably upregulating its gene expression in HaCaT cells already at early time points, i.e., 6 h [27,62]. Among them, PHB/PHOHD fibers displayed interesting outcomes [27]. In this study, we compared PHB/PHOHD with commercial PHA, i.e., PHBHV, electrospun fibers produced under the same conditions, either incorporating or not OLE. Our finding confirmed that PHB/PHOHD fiber meshes, with and without OLE, can induce HBD-2 upregulation and at the same time can downregulate pro-inflammatory cytokines. This capability was not or not sufficiently shown by OLE alone and PHBHV fibers, with and without OLE.

5. Conclusions

Chronic wounds deriving from ulcers from diabetic, vascular and pressure diseases represent a healthcare challenge. To produce advanced wound dressings via electrospinning, we investigated different PHAs either incorporating or not OLE. We demonstrated that OLE can show a different immunomodulatory activity in vitro if administrated directly or upon release by PHA fiber meshes, turning from pro-inflammatory to anti-inflammatory,

and even stimulatory of defensin in the case of PHB/PHOHD scaffolds. Such a diverse behavior can be explained by the longer release time of OLE provided by its incorporation in the polymer matrices, as well as by the combined effect of the fiber topography and chemistry, which ultimately appeared prominent. Having a biocompatible and biodegradable scaffold able to suppress inflammation and stimulate innate immune response would greatly benefit chronic wound care and management.

References

1. Şahin, S.; Bilgin, M. Olive tree (*Olea europaea* L.) leaf as a waste by-product of table olive and olive oil industry: A review. *J. Sci. Food Agric.* **2018**, *98*, 1271–1279. [CrossRef]
2. Romero, M.; Toral, M.; Gómez-Guzmán, M.; Jiménez, R.; Galindo, P.; Sánchez, M.; Olivares, M.; Gálvez, J.; Duarte, J. Antihypertensive effects of oleuropein-enriched olive leaf extract in spontaneously hypertensive rats. *Food Funct.* **2016**, *7*, 584–593. [CrossRef]
3. Susalit, E.; Agus, N.; Effendi, I.; Tjandrawinata, R.R.; Nofiarny, D.; Perrinjaquet-Moccetti, T.; Verbruggen, M. Olive (Olea europaea) leaf extract effective in patients with stage-1 hypertension: Comparison with Captopril. *Phytomedicine* **2011**, *18*, 251–258. [CrossRef]
4. Lockyer, S.; Rowland, I.; Spencer, J.P.E.; Yaqoob, P.; Stonehouse, W. Impact of phenolic-rich olive leaf extract on blood pressure, plasma lipids and inflammatory markers: A randomised controlled trial. *Eur. J. Nutr.* **2017**, *56*, 1421–1432. [CrossRef]
5. Koca, U.; Süntar, I.; Akkol, E.K.; Yilmazer, D.; Alper, M. Wound repair potential of Olea europaea L. leaf extracts revealed by in vivo experimental models and comparative evaluation of the extracts' antioxidant activity. *J. Med. Food* **2011**, *14*, 140–146. [CrossRef]
6. Bulotta, S.; Celano, M.; Lepore, S.M.; Montalcini, T.; Pujia, A.; Russo, D. Beneficial effects of the olive oil phenolic components oleuropein and hydroxytyrosol: Focus on protection against cardiovascular and metabolic diseases. *J. Transl. Med.* **2014**, *12*, 1–9. [CrossRef]
7. Ryu, S.J.; Choi, H.S.; Yoon, K.Y.; Lee, O.H.; Kim, K.J.; Lee, B.Y. Oleuropein suppresses LPS-induced inflammatory responses in RAW 264.7 Cell and zebrafish. *J. Agric. Food Chem.* **2015**, *63*, 2098–2105. [CrossRef]
8. El, S.N.; Karakaya, S. Olive tree (Olea europaea) leaves: Potential beneficial effects on human health. *Nutr. Rev.* **2009**, *67*, 632–638. [CrossRef]
9. De la Ossa, J.G.; Felice, F.; Azimi, B.; Esposito Salsano, J.; Digiacomo, M.; Macchia, M.; Danti, S.; Di Stefano, R. Waste autochthonous tuscan olive leaves (*Olea europaea* var. *Olivastra seggianese*) as antioxidant source for biomedicine. *Int. J. Mol. Sci.* **2019**, *20*, 5918. [CrossRef]
10. Vezza, T.; Algieri, F.; Rodríguez-Nogales, A.; Garrido-Mesa, J.; Utrilla, M.P.; Talhaoui, N.; Gómez-Caravaca, A.M.; Segura-Carretero, A.; Rodríguez-Cabezas, M.E.; Monteleone, G.; et al. Immunomodulatory properties of Olea europaea leaf extract in intestinal inflammation. *Mol. Nutr. Food Res.* **2017**, *61*, 1601066. [CrossRef]

11. Yahfoufi, N.; Alsadi, N.; Jambi, M.; Matar, C. The immunomodulatory and anti-inflammatory role of polyphenols. *Nutrients* **2018**, *10*, 1618. [CrossRef]

12. González, R.; Ballester, I.; López-Posadas, R.; Suárez, M.D.; Zarzuelo, A.; Martínez-Augustin, O.; Sánchez de Medina, F. Effects of flavonoids and other polyphenols on inflammation. *Crit. Rev. Food Sci. Nutr.* **2011**, *51*, 331–362. [CrossRef]

13. Wang, K.; Ping, S.; Huang, S.; Hu, L.; Xuan, H.; Zhang, C.; Hu, F. Molecular Mechanisms Underlying the In Vitro Anti-Inflammatory Effects of a Flavonoid-rich Ethanol Extract from Chinese Propolis (Poplar Type). *Evid. Based Complement. Altern. Med.* **2013**, *2013*, 11. [CrossRef]

14. Magrone, T.; Spagnoletta, A.; Salvatore, R.; Magrone, M.; Dentamaro, F.; Russo, M.A.; Difonzo, G.; Summo, C.; Caponio, F.; Jirillo, E. Olive leaf extracts act as modulators of the human immune response. *Endocrine. Metab. Immune Disord. Drug Targets* **2017**, *18*, 85–93. [CrossRef]

15. Murray, P.J.; Wynn, T.A. Protective and pathogenic functions of macrophage subsets. *Nat. Rev. Immunol.* **2011**, *11*, 723–737. [CrossRef]

16. Azimi, B.; Maleki, H.; Zavagna, L.; De la Ossa, J.G.; Linari, S.; Lazzeri, A.; Danti, S. Bio-based electrospun fibers for wound healing. *J. Funct. Biomater.* **2020**, *11*, 67. [CrossRef]

17. Larsen, S.B.; Cowley, C.J.; Fuchs, E. Epithelial cells: Liaisons of immunity. *Curr. Opin. Immunol.* **2020**, *62*, 45–53. [CrossRef]

18. Raza, Z.A.; Abid, S.; Banat, I.M. Polyhydroxyalkanoates: Characteristics, production, recent developments and applications. *Int. Biodeterior. Biodegrad.* **2018**, *126*, 45–56. [CrossRef]

19. Nigmatullin, R.; Thomas, P.; Lukasiewicz, B.; Puthussery, H.; Roy, I. Polyhydroxyalkanoates, a family of natural polymers, and their applications in drug delivery. *J. Chem. Technol. Biotechnol.* **2015**, *90*, 1209–1221. [CrossRef]

20. Francis, L.; Meng, D.; Knowles, J.; Keshavarz, T.; Boccaccini, A.R.; Roy, I. Controlled Delivery of Gentamicin Using Poly(3-hydroxybutyrate) Microspheres. *Int. J. Mol. Sci.* **2011**, *12*, 4294–4314. [CrossRef]

21. Azimi, B.; Milazzo, M.; Lazzeri, A.; Berrettini, S.; Uddin, M.J.; Qin, Z.; Buehler, M.J.; Danti, S. Electrospinning Piezoelectric Fibers for Biocompatible Devices. *Adv. Healthc. Mater.* **2020**, *9*, 1–39. [CrossRef] [PubMed]

22. Salomone, R.; Ioppolo, G. Environmental impacts of olive oil production: A Life Cycle Assessment case study in the province of Messina (Sicily). *J. Clean. Prod.* **2012**, *28*, 88–100. [CrossRef]

23. Rombaut, N.; Tixier, A.-S.; Bily, A.; Chemat, F. Green extraction processes of natural products as tools for biorefinery. *Biofuels Bioprod. Bioref.* **2014**, *8*, 530–544. [CrossRef]

24. Benavente-García, O.; Castillo, J.; Lorente, J.; Ortuño, A.; Del Rio, J.A. Antioxidant activity of phenolics extracted from Olea europaea L. leaves. *Food Chem.* **2000**, *68*, 457–462. [CrossRef]

25. Alessandri, S.; Ieri, F.; Romani, A. Minor polar compounds in extra virgin olive oil: Correlation between HPLC-DAD-MS and the Folin-Ciocalteu spectrophotometric method. *J. Agric. Food Chem.* **2014**, *62*, 826–835. [CrossRef]

26. Doğan, G.; Başal, G.; Bayraktar, O.; Ozyildiz, F.; Uzel, A.; Erdoğan, I. Bioactive Sheath/Core nanofibers containing olive leaf extract. *Microsc. Res. Tech.* **2016**, *79*, 38–49. [CrossRef]

27. Chuysinuan, P.; Thanyacharoen, T.; Techasakul, S.; Ummartyotin, S. Electrospun characteristics of gallic acid-loaded poly vinyl alcohol fibers: Release characteristics and antioxidant properties. *J. Sci. Adv. Mater. Devices.* **2018**, *3*, 175–180. [CrossRef]

28. Frykberg, R.G.; Banks, J. Challenges in the Treatment of Chronic Wounds. *Adv. Wound Care* **2015**, *4*, 560–582. [CrossRef]

29. Dhivya, S.; Padma, V.V.; Santhini, E. Wound dressings—A review. *Biomedicine* **2015**, *5*, 24–28. [CrossRef]

30. Danti, S.; D'Alessandro, D.; Mota, C.; Bruschini, L.; Berrettini, S. Applications of Bioresorbable Polymers in Skin and Eardrum. In *Bioresorbable Polymers for Biomedical Applications: From Fundamentals to Translational Medicine*; Elsevier: Amsterdam, The Netherlands, 2017; pp. 423–444. ISBN 9780081002667.

31. Azimi, B.; Thomas, L.; Fusco, A.; Kalaoglu-Altan, O.I.; Basnett, P.; Cinelli, P.; De Clerck, K.; Roy, I.; Donnarumma, G.; Coltelli, M.-B.; et al. Electrosprayed chitin nanofibril/electrospun polyhydroxyalkanoate fiber mesh as functional nonwoven for skin application. *J. Funct. Biomater.* **2020**, *11*, 62. [CrossRef] [PubMed]

32. Lizarraga-Valderrama, L.R.; Taylor, C.S.; Claeyssens, F.; Haycock, J.W.; Knowles, J.C.; Roy, I. Unidirectional neuronal cell growth and differentiation on aligned polyhydroxyalkanoate blend microfibres with varying diameters. *J. Tissue Eng. Regen. Med.* **2019**, *13*, 1581–1594. [CrossRef]

33. Ching, K.Y.; Andriotis, O.G.; Li, S.; Basnett, P.; Su, B.; Roy, I.; Tare, R.S.; Sengers, B.G.; Stolz, M. Nanofibrous poly(3-hydroxybutyrate)/poly(3-hydroxyoctanoate) scaffolds provide a functional microenvironment for cartilage repair. *J. Biomater. Appl.* **2016**, *31*, 77–91. [CrossRef] [PubMed]

34. Fong, H.; Chun, I.; Reneker, D.H. Beaded Nanofibers Formed during Electrospinning. *Polymer* **1999**, *40*, 4585–4592. [CrossRef]

35. Liu, Y.-H.; He, J.-H.; Yu, J.Y.; Zeng, H.-M. Controlling numbers and sizes of beads in electrospun nanofibers. *Polym. Int.* **2008**, *57*, 632–636. [CrossRef]

36. Gaharwar, A.K.; Mihaila, S.M.; Kulkarni, A.A.; Patel, A.; Di Luca, A.; Reis, R.L.; Gomes, M.E.; van Blitterswijk, C.; Moroni, L.; Khademhosseini, A. Amphiphilic beads as depots for sustained drug release integrated into fibrillar scaffolds. *J. Control. Release* **2014**, *187*, 66–73. [CrossRef] [PubMed]

37. Özcan, M.M.; Matthäus, B. A review: Benefit and bioactive properties of olive (Olea europaea L.) leaves. *Eur. Food Res. Technol.* **2017**, *243*, 89–99. [CrossRef]

38. Nediani, C.; Ruzzolini, J.; Romani, A.; Calorini, L. Oleuropein, a bioactive compound from Olea europaea L., as a potential preventive and therapeutic agent in non-communicable diseases. *Antioxidants* **2019**, *8*, 578. [CrossRef]

39. Estruch, R. Effects of a Mediterranean-style diet on cardiovascular risk factors: A randomized trial. *Ann. Intern. Med.* **2006**, *145*, 1–11. [CrossRef]
40. Miles, E.A.; Zubouli, P.; Calder, P.C. Differential anti-inflammatory effects of phenolic compounds from extra virgin olive oil identified in human whole blood cultures. *Nutrition* **2005**, *21*, 389–394. [CrossRef]
41. De Cicco, P.; Maisto, M.; Tenore, G.C.; Ianaro, A. Olive Leaf Extract, from *Olea europaea* L., Reduces Palmitate-Induced Inflammation via Regulation of Murine Macrophages Polarization. *Nutrients* **2020**, *12*, 3663. [CrossRef]
42. Gordon, S.; Martinez, F.O. Alternative activation of macrophages: Mechanism and functions. *Immunity* **2010**, *32*, 593–604. [CrossRef] [PubMed]
43. Liu, Y.; McKeever, L.C.; Malik, N.S.A. Assessment of the antimicrobial activity of olive leaf extract against foodborne bacterial pathogens. *Front. Microbiol.* **2017**, *8*, 113. [CrossRef]
44. De La Ossa, J.G.; El Kadri, H.; Gutierrez-Merino, J.; Wantock, T.; Harle, T.; Seggiani, M.; Danti, S.; Di Stefano, R.; Velliou, E. Combined antimicrobial effect of bio-waste olive leaf extract and remote cold atmospheric plasma effluent. *Molecules* **2021**, *26*, 1890. [CrossRef]
45. Chew, S.A.; Danti, S. Biomaterial-based implantable devices for cancer therapy. *Adv. Healthc. Mater.* **2017**, *6*, 1600766. [CrossRef] [PubMed]
46. Ricci, C.; Trombi, L.; Soriga, I.; Piredda, F.; Milazzo, M.; Stefanini, C.; Bruschini, L.; Perale, G.; Pertici, G.; Danti, S. Investigating the microenvironmental effects of scaffold chemistry and topology in human mesenchymal stromal cell/polymeric hollow microfiber constructs. *Biomed. Sci. Eng.* **2016**, *1*, 1. [CrossRef]
47. Duval, K.; Grover, H.; Han, L.-H.; Mou, Y.; Pegoraro, A.F.; Fredberg, J.; Chen, Z. Modeling physiological events in 2D vs. 3D cell culture. *Physiology* **2017**, *32*, 266–277. [CrossRef] [PubMed]
48. Milazzo, M.; Gallone, G.; Marcello, E.; Mariniello, D.; Bruschini, L.; Roy, I.; Danti, S. Biodegradable polymeric micro/nano-structures with intrinsic antifouling/antimicrobial properties: Relevance in damaged skin and other biomedical applications. *J. Funct. Biomater.* **2020**, *11*, 60. [CrossRef]
49. Esposito, E.; Cuzzocrea, S. TNF-alpha as a therapeutic target in inflammatory diseases, ischemia-reperfusion injury and trauma. *Curr. Med. Chem.* **2009**, *16*, 3152–3167. [CrossRef]
50. Coondoo, A. The role of cytokines in the pathomechanism of cutaneous disorders. *Indian J. Dermatol.* **2012**, *57*, 90–96. [CrossRef]
51. Tanaka, T.; Narazaki, M.; Masuda, K.; Kishimoto, T. Regulation of IL-6 in Immunity and Diseases. In *Regulation of Cytokine Gene Expression in Immunity and Diseases*; Ma, X., Ed.; Advances in Experimental Medicine and Biology; Springer: Dordrecht, The Netherlands, 2016; Volume 941.
52. Harada, A.; Sekido, N.; Akahoshi, T. Essential involvement of interleukin-8 (IL-8) in acute inflammation. *J. Leukoc. Biol.* **1994**, *56*, 559–564. [CrossRef]
53. Maaz Arif, M.; Khan, S.M.; Gull, N.; Tabish, T.A.; Zia, S.; Ullah Khan, R.; Awais, S.M.; Arif Butt, M. Polymer-based biomaterials for chronic wound management: Promises and challenges. *Int. J. Pharm.* **2021**, *598*, 120270. [CrossRef] [PubMed]
54. Wolcott, R.D.; Rhoads, D.D.; Dowd, S.E. Biofilms and chronic wound inflammation. *J. Wound Care* **2008**, *17*, 333–341. [CrossRef] [PubMed]
55. Saino, E.; Focarete, M.L.; Gualandi, C.; Emanuele, E.; Cornaglia, A.I.; Imbriani, M.; Visai, L. Effect of electrospun fiber diameter and alignment on macrophage activation and secretion of proinflammatory cytokines and chemokines. *Biomacromolecules* **2011**, *12*, 1900–1911. [CrossRef] [PubMed]
56. Wanke, I.; Steffen, H.; Christ, C.; Krismer, B.; Götz, F.; Peschel, A.; Peschel, A.; Schaller, M.; Schittek, B. Skin commensals amplify the innate immune response to pathogens by activation of distinct signaling pathways. *J. Investig. Dermatol.* **2011**, *131*, 382–390. [CrossRef]
57. Donnarumma, G.; Paoletti, I.; Fusco, A.; Perfetto, B.; Buommino, E.; de Gregorio, V.; Baroni, A. β-Defensins: Work in Progress. *Adv. Exp. Med. Bio.I* **2016**, *901*, 59–76. [CrossRef]
58. Coltelli, M.-B.; Aliotta, L.; Vannozzi, A.; Morganti, P.; Panariello, L.; Danti, S.; Neri, S.; Fernandez-Avila, C.; Fusco, A.; Donnarumma, G.; et al. Properties and skin compatibility of films based on poly(lactic acid) (PLA) bionanocomposites incorporating chitin nanofibrils (CN). *J. Funct. Biomater.* **2020**, *11*, 21. [CrossRef]
59. Danti, S.; Azimi, B.; Candito, M.; Fusco, A.; Sorayani Bafqi, M.S.; Ricci, C.; Milazzo, M.; Cristallini, C.; Latifi, M.; Donnarumma, G.; et al. Lithium niobate nanoparticles as biofunctional interface material for inner ear devices. *Biointerphases* **2020**, *15*, 031004. [CrossRef]
60. Danti, S.; Trombi, L.; Fusco, A.; Azimi, B.; Lazzeri, A.; Morganti, P.; Coltelli, M.-B.; Donnarumma, G. Chitin nanofibrils and nanolignin as functional agents in skin regeneration. *Int. J. Mol. Sci.* **2019**, *20*, 2669. [CrossRef]
61. Gigante, V.; Coltelli, M.-B.; Vannozzi, A.; Panariello, L.; Fusco, A.; Trombi, L.; Donnarumma, G.; Danti, S.; Lazzeri, A. Flat die extruded biocompatible poly(lactic acid) (PLA)/poly(butylene succinate) (PBS) based films. *Polymers* **2019**, *11*, 1857. [CrossRef] [PubMed]
62. Teno, J.; Pardo-Rodriguez, M.; Hummel, N.; Bonin, V.; Fusco, A.; Ricci, C.; Donnarumma, G.; Coltelli, M.-B.; Danti, S.; Lagaron, J.M. Preliminary studies on an innovative bioactive skin soluble beauty mask made by combining electrospinning and dry powder impregnation. *Cosmetics* **2020**, *7*, 96. [CrossRef]